IOSR Journal of Electronics and Communication Engineering (IOSR-JECE)
e-ISSN: 2278-2834,p- ISSN: 2278-8735.Volume 14, Issue 2, Ser. II (Mar.-Apr. 2019), PP 22-29
www.iosrjournals.org

Evaluation of Quality Parameters for Medical Image Fusion

H.Devanna[1], G.A.E. Satish Kumar[2], G.Mamatha[3]
[1]*Research Scholar, Department of ECE, JNTUA, Ananthapuramu, AP, India*
[2]*Professor, Department of ECE, Vardhaman College of Engineering, Hyderabad, Telangana, India*
[3]*Assistant Professor, Department of ECE, JNTU College of Engineering, Anantapuramu, A.P, India*
Corresponding Author: H.Devanna

Abstract: *In this paper, we evaluate three variants of new quality parameters for medical image fusion. The aims of our evaluated parameters are based on an image quality index. We perform several simulations which show that our parameters are compliant with subjective evaluations and can therefore be used to compare different image fusion methods or to find the best parameters for a given fusion algorithm.*

Keywords: *Medical image fusions, DWT, curvelet transform, contourlet transform*

Date of Submission: 15-04-2019 Date of acceptance: 30-04-2019

I. Introduction

The rapid and significant advancements in medical imaging technologies and sensors, lead to new uses of medical images in various healthcare and bio-medical applications including diagnosis, research, treatment and education etc. Different modalities of medical images reflect different information of human organs and tissues, and have their respective application ranges. For instance, structural images like magnetic resonance imaging (MRI), computed tomography (CT), ultrasonography (USG) and magnetic resonance angiography (MRA) etc. provide high-resolution images with excellent anatomical detail and precise localization capability. Whereas, functional images such as position emission tomography (PET), single-photon emission computed tomography (SPECT) and functional MRI (fMRI) etc., provide low-spatial resolution images with functional information, useful for detecting cancer and related metabolic abnormalities. A single modality of medical image cannot provide comprehensive and accurate information. Therefore, it is necessary to correlate one modality of medical image to another to obtain the relevant information. Moreover, the manual process of integrating several modalities of medical images is rigorous, time consuming, costly, subject to human error, and requires years of experience. Therefore, automatically combining multimodal medical images through image fusion (IF) has become the main research focus in medical image processing [1], [2].

Image fusion is a methodology concerned with the integration of multiple images, e.g. derived from different sensors, into a composite image that is more suitable for the purposes of human visual perception or computer-processing tasks. The widespread use of image fusion methods, in military applications, in surveillance, in medical diagnostics, etc, has led to a rising demand of pertinent quality assessment tools in order to compare the results obtained with existinting method or to obtain an optimal setting of parameters..Quality assessment of fused images is often carried out by human visual inspection [3]. Objective performance assessment is a difficult issue due to the variety of different application requirements and the lack of a clearly defined ground-truth. Indeed, various fusion algorithms presented in the literature [4] have been evaluated by constructing some kind of ideal fused image and using it as a reference for comparing with the experimental fused results [5, 6]. Mean squared error (MSE) based metrics are widely used for these comparisons. A restricted number of objective fusion performance measures have been proposed where the knowledge of ground-truth is not assumed. Xydeas and Petrović [7] propose a metric that evaluates the relative amount of edge information that is transferred from the input images to the fused image. In mutual information is employed for evaluating fusion performance.

II. Literature Survey

Based on the methodology of fusion process, the earlier approaches are categorized into two categories as pixel based image fusion and transform based image fusion. The simplest spatial-based method is to take the average of the input images pixel by pixel. However, along with its simplicity, this method leads to several undesirable side effects, such as reduced contrast. To improve the quality of fused image, various approaches are propose in earlier based on the block division if source images. Here the source images are initially decomposed into blocks and the optimal blocks are chosen for the fusion. The motivation of this methodology lies in the fact that an optimized block size could be more effective than a fixed block size. This type of

algorithm may not only improve the convergence between each pixel in the fused image but may also easily produce block effect. And also the finding of a suitable block-size is a problem. A large block is more likely to contain portions from both focused and defocused regions. This may lead to selection of considerable amount of defocused regions. On the other hand, small blocks do not vary much in relative contrast and hence difficult to choose from. Moreover, small blocks are more affected by misregistration problems. To solve these issues, a novel optimal method for multi-focus image fusion using differential evolution algorithm is presented in [8]. The source images are first decomposed into blocks. Then, the sharper blocks are selected by employing a sharpness criterion function. The selected blocks are finally combined to construct the fused image. Similarly the quad-tree structure method is proposed in [9] to solve the problem of how to determine the size of sub-blocks. Further two more block based approaches are proposed in [10] and [11] to evaluate the local content (sharp) information of the input source images by which the blocking effect in the fused image will reduces efficiently. Though these approaches achieved an efficient fusion performance, the blocking effect is not eliminated completely. Another region segmentation approach is proposed in [12] to find the regions through the morphological filtering. Then, image matting technique is applied to obtain the accurate focused region of each source image. Finally, the focused regions are combined together to construct the fused image. Through image matting, the proposed fusion algorithm combines the focus information and the correlations between nearby pixels together [13].However, these methods may generate artificial information and discontinuous phenomena at the boundaries of focused regions because the boundary cannot be determined accurately. These effects will reduce the visual fidelity of the fused image.

To achieve more efficient results, the medical image fusion is shifted towards the transform domain through the accomplishment of MST, including the discrete wavelet transform (DWT) [3, 7, and 37], framelet transform [14], contourlet transform [15], and non-sub sampled contourlet transform (NSCT) [1, 4, 6]. By focusing on the properties of wavelet filters, some extended wavelet based image fusion approaches are proposed based on Wavelet Packet Transform (WPT) [16] and Wavelet Frame Transform (WFT) [17]. Wavelet transform suffers from lack of shift invariance & poor directionality and Stationary Wavelet Transform and Wavelet Packet Transform overcome these disadvantages. Further the wavelet frame transform is aliasing free and translation invariant. In [18], a new image fusion approach is proposed based on the Discrete Wavelet transform and type-2 fuzzy logic. Here the main is avoiding the extra noise in the fused image. In this method, source images are decomposed into low-level subband, high-level subbands using DWT. Next, low-level sub-images are fused using type-2 fuzzy fusion rule and high-level sub-images are fused using average fusion rule. Finally, inverse DWT is applied on the fused components to obtain the fused image. However, wavelet transform cannot effectively represent the line singularities and plane singularities of the images.

To overcome these shortcomings with wavelet transform, the further research is focused through the contourlet transform and Non-Subsampled Contourlet Transform. The main difference between the Contourlet Transform and Non-Subsampled Contourlet Transform is shift invariant property. Recently Hui Huang et al., [19] propose a novel image fusion algorithm that combines nonlinear approximation of contourlet transform [20] with image regional features. The most important coefficient bands of the contourlet sparse matrix are retained by nonlinear approximation. However, the up- and down-sampling process of Contourlet decomposition and reconstruction results in the CT lacking shift-invariance and having pseudo-Gibbs phenomena in the fused image. The Non-Subsampled Contourlet Transform inherits the advantages of Contourlet Transform, while also possessing shift-invariance and effectively suppressing Pseudo-Gibbs phenomena. Hence Non-Subsampled Contourlet Transform is chosen as a prominent transform for multimodal medical image fusion and so many approaches are proposed based on Non-Subsampled Contourlet Transform [22-24].

III. Non-Subsampled Contourlet Transform

The Non-Subsampled Contourlet Transform [28] is developed based on the theory of contourlet transform only. Non-Subsampled Contourlet Transform is advantageous in the provision of shift invariance, boosts the directional selectivity and reduces the significance of pseudo-Gibbs phenomena effectively. The decomposition process of the Non-Subsampled Contourlet Transform is divided into two phases, i.e., the Non-sub Sampled Pyramids (NSP) and the Non-sub Sampled Directional Filter Bank (NSDFB). The former performs multiscale decomposition and the later provide direction decomposition. The NSP divides image into a low frequency sub band and a high frequency sub band in each level. For a given k level of decomposition the NSP generates k+1 sub-band images, consists of one low frequency sub band image and the remaining k sub band images are high frequency sub band images. Subsequently, the NSDFB divides the high frequency sub band image into directional sub band images. For a given level of decomposition l, 2l directional sub band images will be obtained for a particular high frequency sub band image.

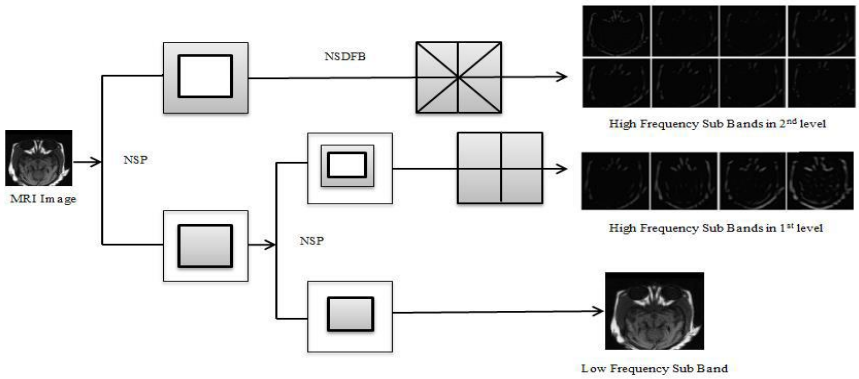

Figure.1 MRI Image decomposition through Non-Subsampled Contourlet Transform for two levels

After the low frequency component is decomposed iteratively by the same way, an image is finally decomposed into one low frequency sub image and a series of high frequency directional subband images ($\Sigma 2^{ljkj}$=1), where in ^{lj}denotes the number of decomposition directions at the j scale. Figure.1 represents the schematic of Non-Subsampled Contourlet Transform. Hence the NSDFB offers more accurate directional information through the bands obtained in multi-directional orientations to produce more accurate results. Thus, the Non-Subsampled Contourlet Transform ensures the optimal frequency selectivity and also an essential shift invariance property on the aspect of non-subsampled operation. Here an important to note that is the dimensions of obtained sub-images is in identical fashion. In addition, the Non-Subsampled Contourlet Transform also reduces the misregistration effects over the obtained results. Thus, the proposed model considered Non-Subsampled Contourlet Transform for medical image effusion.

IV. A New Fusion Quality Parameters

We would like to present a brief introduction to the image quality index. Given two real-valued sequences x = (x_1,x_2 ….x_n) and y = (y_1,y_2 ….y_n). Let $\bar{x}$ denotes the mean of x, let $\sigma_x{}^2$ and σ_{xy} be the variance of x and covariance of x, y respectively.

$$\sigma_x{}^2 = \frac{1}{n-1}\sum_{i=1}^{n}(x_i - \bar{x})^2 \, , \sigma_{xy} = \frac{1}{n-1}\sum_{i=1}^{n}(x_i - \bar{x})(y_i - \bar{y})$$

Now we calculate

$$Q_0 = \frac{4\sigma_{xy}\,\bar{x}\bar{y}}{(\bar{x}^2+\bar{y}^2)(\sigma_x{}^x+\sigma_y{}^2)} \qquad (1)$$

This can be decomposed as

$$Q_0 = \frac{\sigma_{xy}}{\sigma_x\sigma_y}\frac{2\bar{x}\bar{y}}{\bar{x}^2+\bar{y}^2}\frac{2\sigma_x\sigma_y}{\sigma_x{}^2+\sigma_y{}^2} \qquad (2)$$

In above equation the first component is the correlation coefficient between x and y. The value $Q_0 = Q_0(x, y)$ is a measure for the similarity of the vectors x and y and takes values between -l and 1.

Since image signals are generally non-stationary, it is more appropriate to measure the image quality index Q_0 over local regions and then combine the different results into a single measure. Note that in this case the values x_i and $y_i$are positive grey-scale values. Now the second component corresponds to the luminance distortion and it has a dynamic range of [0, l]. The third factor is measures the contrast distortion and its range is also [0, 1]. The maximum value $Q_0 = 1$ is achieved when x and y are identical.

(i)LOACA QUALITY INDEX (Q_0): We propose to use a sliding window approach, starting from the top-left corner of the two images A, B, a sliding window of fixed size (with n pixels) moves pixel by pixel over the entire image until the bottom-right corner is reached. For each window w, the local quality index $Q_0(A, B|\omega)$ is computed for the values A (i, j) and B (i,j) where pixels (i, j) lie in the sliding window w. Finally, the overall image quality index Q_0 is computed by averaging all local quality indices:

$$Q_0\,(a, b) = \frac{1}{|W|}\sum_{\omega\varepsilon W} Q_0(A, B|\omega) \qquad (3)$$

Where W is the family of all windows and $|W|$is the cardinality of W

We have to compare their quality index with existing image measures such as the MSE. Their main conclusion was that their new index out performs the MSE, and they believe this to be due to the index's ability of measuring structural distortions, in contrast to the MSE which is highly sensitive to the L^2 energy of errors.

We use the image quality index Q_0 defined in (3) to define a quality index Q (A, B, F) for image fusion. Here A, B are two input images and F is the fused image. The index Q (A, B, F) should express the 'quality' of the fused image given the inputs A,B.

We denote by $s(A|\omega)$ some saliency of image A in window ω. It should reflect the local relevance of image a within the window ω, and it may depend on contrast, sharpness, or entropy. Given the local saliencies $s(A|\omega)$ and $s(B|\omega)$ of the two input images A and B. we compute a local weight $\lambda(\omega)$between 0 and 1 indicating the relative importance of image A compared to image B, the larger $\lambda(\omega)$,the more weight is given to image A. A typical choice for $\lambda(\omega)$is

$$\lambda(\omega)= \frac{s(A|\omega)}{s(A|\omega)+s(B|\omega)} \qquad (4)$$

Now we define the fusion quality index Q(A, B, F) as

$$Q(A,B,F) = \frac{1}{|W|}\sum_{\omega\varepsilon W} \left(\lambda(\omega)Q_0(A,F|\omega) + \big(1-\lambda(\omega)\big)Q_0(B,F|\omega)\right) \qquad (5)$$

Thus, in regions where image A has a large saliency compared to B, the quality index Q (A, B, F) is mainly determined by the input image A. On the other hand, in regions where the saliency of B is much larger than that of A, the index Q (A, B, F) is determined mostly by input image B.

(ii) WEIGHTED FUSION QUALITY INDEX (Q_W): our model has produced a quality index which gives an indication of how much of the salient information contained in each of the input images has been transferred into the fused image without introducing distortions. However, the different quality measures obtained within each window have been treated equally. This is in contrast with the human visual system (HVS) which is known to give higher importance to visually salient regions in an image. We now define another variant of the fusion quality index by giving more weight to those windows where the saliency of the input images is higher. These correspond to areas which are likely to be perceptually important parts of the underlying scene. Therefore the quality of the fused image in those areas is of more importance when determining the overall quality index. The overall saliency of a window is defined as

$$C(\omega) = \max\left(s(A|\omega), s(B|\omega)\right)$$

The weighted fusion quality index is then defined as

$$Q_W(A,B,F) = \sum_{\omega\varepsilon W} c(\omega)\left(\lambda(\omega)Q_0(A,F|\omega) + \big(1-\lambda(\omega)\big)Q_0(B,F|\omega)\right) \qquad (6)$$

$$\text{Where } c(\omega) = C(\omega) / \left(\sum_{\omega'\varepsilon W} C(\omega')\right)$$

There are various other ways to compute the weights c(ω), (for example, we could define $C(\omega) = s(A|\omega) + s(B|\omega)$), but we have found that the choice made here is a good indicator of important areas in the input images.

(iii) EDGE- DEPENDENT FUSION QUALITY INDEX (Q_E): We define one final modification of the fusion quality index that takes into account some aspect of the HVS, namely the importance of edge information. Note that we can evaluate Q_w in (6) using 'edge images' instead of the original grey-scale images A, Band F. Let us denote the edge image corresponding with A byA'. Now we combine Q_w(A, B, F) and Q_w(A' , B',F') into a so-called **edge-dependent fusion quality index** by

$$Q_E(A,B,F) = Q_W(A,B,F)\,.\,Q_W(A',B',F')^{\alpha} \qquad (7)$$

Where α is a parameter that expresses the contribution of the edge images compared to the original images

V. Simulation Results

This section illustrates the details of performance evaluation of proposed framework quantitatively and qualitatively. To verify the performance of proposed approach, an extensive simulation is carried out over various types of medical images and like MRI, CT, MR-T1 and MR-T2. Here the source images of size 256*256 are considered and the simulation is carried through MATLAB software. The obtained fused images are shown in Figs. 2-4.

In this paper, three objective evaluation measurements parameters are adopted to evaluate the fusion performance. There are local quality index ($Q0$) [24], weighted fusion quality index (QW) [24], edge-dependent fusion quality index (QE) [24], the range of $Q0$, QW, QE, lies between 0 and 1.

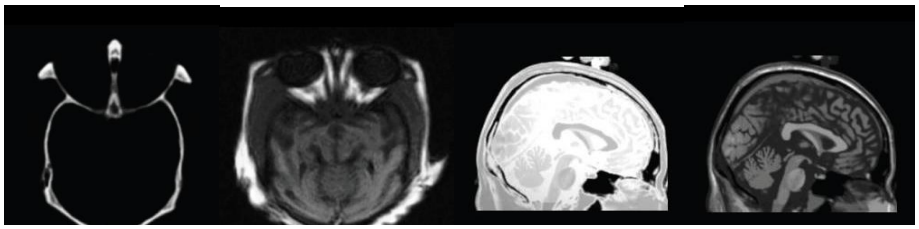

(a) (b) (c) (d)

Figure.2. Test images set 1 (a) CT (b) MRI
Test Images set 2 (c) CT (d) MRI

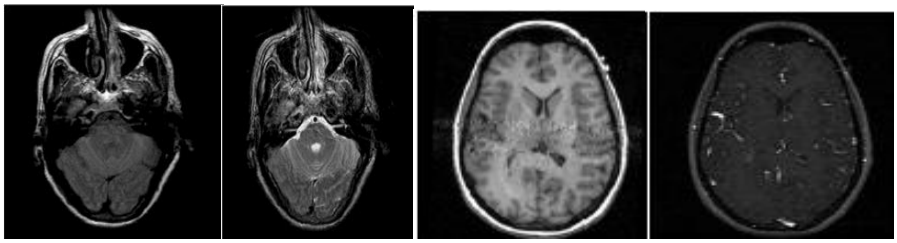

(e) (f) (g) (h)

Figure.3. Test images set 3 (e) MR-T1 (f) MR-T2
Test Images set 4 (g) MR-T1 (h) MR-T2

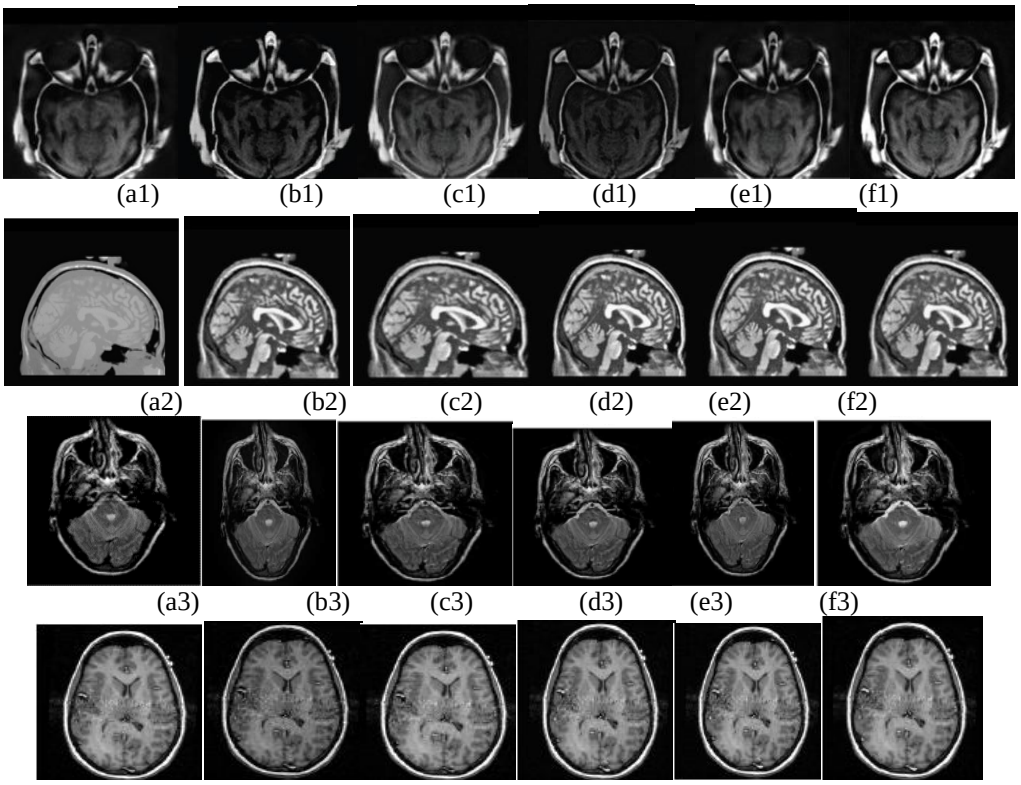

(a1) (b1) (c1) (d1) (e1) (f1)

(a2) (b2) (c2) (d2) (e2) (f2)

(a3) (b3) (c3) (d3) (e3) (f3)

Fig.4. Fused images by a1-a4 DWT[3],b1-b4 CT[11],c1-c4 NSCT[16],d1-d4[25], e1-e4 NSCT[26] and f1-f4 Proposed approach.

Table.1. Local quality index (Q_0)

Test samples	DWT[3]	CT[11]	NSCT-[16]	NSCT-2[25]	NSCT-3[26]	Proposed
Image dataset1 (CT& MRI)	0.6142	0.6152	0.6178	0.6205	0.6220	**0.6233**
Image dataset2 (CT& MRI)	0.7360	0.7370	0.7396	0.7423	0.7438	**0.7451**
Image dataset1 (MR-T1&MR-T2)	0.7698	0.7708	0.7734	0.7761	0.7776	**0.7789**
Image dataset1 (MR-T1&MR-T2)	0.6451	0.6461	0.6487	0.6514	0.6529	**0.6542**

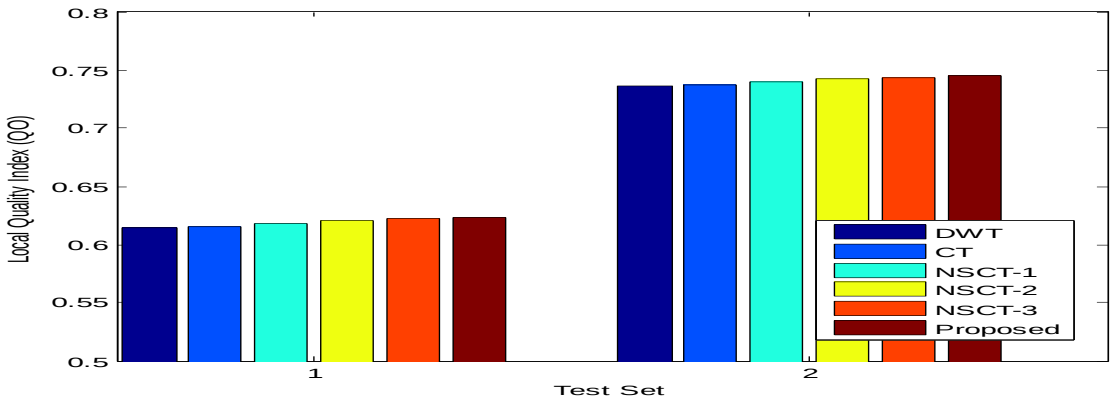

Fig 5. Local quality index (Q_0) observation

Table.2. Weighted fusion quality index (Q_w)

Test samples	DWT[3]	CT[11]	NSCT-[16]	NSCT-2[25]	NSCT-3[26]	Proposed
Image dataset1 (CT& MRI)	0.7237	0.7322	0.7338	0.7369	0.7402	**0.7418**
Image dataset2 (CT& MRI)	0.7155	0.7240	0.7256	0.7287	0.7320	**0.7336**
Image dataset1 (MR-T1&MR-T2)	0.7037	0.7122	0.7138	0.7169	0.7202	**0.7218**
Image dataset1 (MR-T1&MR-T2)	0.7931	0.8016	0.8032	0.8063	0.8096	**0.8112**

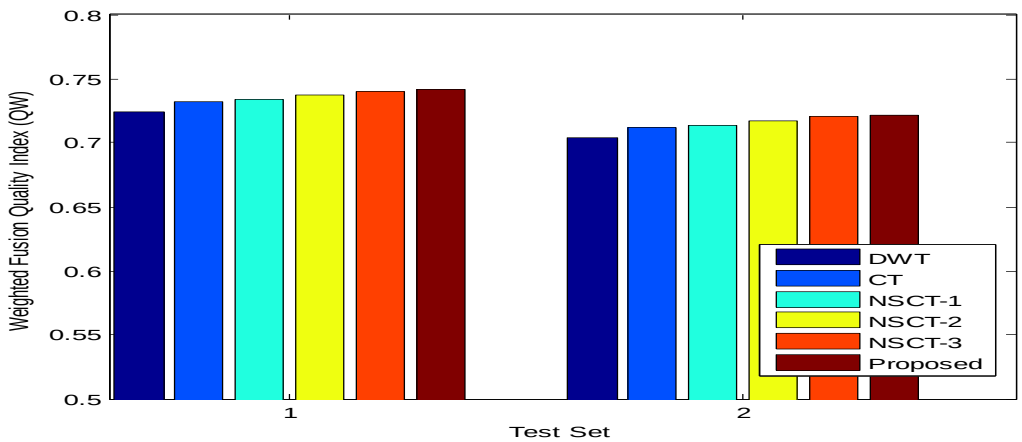

Fig.6. Weighted fusion quality index (Q_w) observation

Table.3. Edge-dependent fusion quality index (Q_E)

Test samples	DWT[3]	CT[11]	NSCT-[16]	NSCT-2[25]	NSCT-3[26]	Proposed
Image dataset1 (CT& MRI)	0.5492	0.5574	0.5599	0.5601	0.5628	**0.5667**
Image dataset2 (CT& MRI)	0.6573	0.6655	0.6680	0.6682	0.6709	**0.6748**
Image dataset1 (MR-T1&MR-T2)	0.7048	0.7130	0.7155	0.7157	0.7184	**0.7223**
Image dataset1 (MR-T1&MR-T2)	0.5972	0.6054	0.6079	0.6081	0.6108	**0.6147**

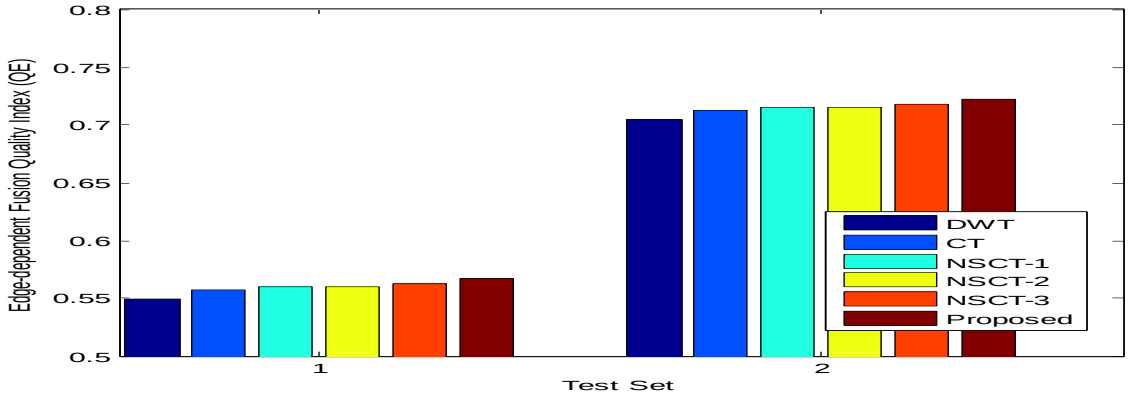

Fig.7.Edge-dependent fusion quality index (Q_E) observation

VI. Conclusions

In this paper we have discussed some new objective quality measures for image fusion. Our measures are easy to calculate and applicable to various input modalities. In particular, our measures give good results on variable quality input images since it takes into account the locations as well as the magnitude of the distortions. There are several areas in which our quality measures can be improved or extended. From the above analysis, it can be observed that the proposed attained a greatest improvement in the calculated quality parameters give better than the existed results. In the future, we can be extended to accomplish through a new metrics based on the band selection approach by which Quality enhancement in the fused image.

References

[1]. B. Solaiman, R. Debon, F. Pipelier, J. M. Cauvin, and C. Roux, Information fusion: Application to data and model fusion for ultrasound image segmentation, IEEE TBME, vol. 46, no. 10, pp. 1171–1175, 1999.
[2]. B. V. Dasarathy, Editorial: Information fusion in the realm of medical applications-a bibliographic glimpse at its growing appeal, Information Fusion 13 (1) (2012) 1–9.
[3]. A. Toet and E. M. Franken, "Perceptual evaluation of different image fusion schemes," Displays, vol. 24, no, l , pp. 25—37, February 2003.
[4]. G.Piella, "A general framework for multiresolution image fusion: from pixels to regions," to appear in Information Fusion, 2003.
[5]. Li, B. S. Manjunath, and S. K. Mitra, "Multisensory image fusion using the wavelet transform," Graphical Models and Image Processing, vol. 57, no. 3, pp. 235—245, May 1995
[6]. C. Xydeas and V. PetroviC, "Objective pixel-level image fusion performance measure,'' in Proceedings of SPIE, April 2000, vol. 4051, pp. 88-99.
[7]. G. H. Qu, D. L. Zhang, and P. F. Yan, "Medical image fusion by wavelet transform modulus maxima," Journal of the Optical ociery of America, vol. 9, no. 4, pp. 184-1 90, 2001.
[8]. V. Aslantas and R. Kurban, "Fusion of multi-focus images using differential evolution algorithm", Expert Syst. Appl., Vol. 37, No. 12, pp. 8861–8870, 2010.
[9]. I. De and B. Chanda, "Multi-focus image fusion using a morphologybased focus measure in a quad- tree structure", Inf. Fusion, Vol. 14, Vo. 2, pp. 136–146, 2013.
[10]. S. Li, J. T. Kwok, and Y. Wang, "Multi-focus image fusion using artificial neural networks", Pattern Recognit. Lett., Vol. 23, No. 8, pp. 985–997, 2002.
[11]. J. Tian, L. Chen, L. Ma, and W. Yu, "Multi-focus image fusion using a bilateral gradient-based sharpness criterion", Opt. Commun., Vol. 284, No. 1, pp. 80–87, 2011.
[12]. S. Li, X. Kang, J. Hu, and B. Yang, "Image matting for fusion of multi-focus images in dynamic scenes", Inf. Fusion, Vol. 14, No. 2, pp. 147–162, 2013.
[13]. Y. Liu, J. Jin, Q. Wang, Y. Shen, and X. Dong, "Region level based multi-focus image fusion using quaternion wavelet and normalized cut", Signal Process., Vol. 97, pp.9–30, 2014.
[14]. G. Bhatnagar, Q. M. J. Wu, and Z. Liu, "Human visual system inspired multi-modal medical image fusion framework", Expert Systems with Applications, Vol. 40, No. 5, pp. 1708–1720, 2013.

[15]. L. Yang, B. L. Guo, and W. Ni, "Multimodality medical image fusion based on multiscale geometric analysis of contourlet transform", Neuro computing, Vol. 72, No. 1-3, pp. 203– 211, 2008.
[16]. K. Kannan, S. A. Perumal, and K. Arulmozhi, "Area level fusion of multi-focused images using multi-stationary wavelet packet transform", Int. J. Comput. Appl., Vol. 2, No. 1, pp. 88–95, 2010.
[17]. S. Li, J. T. Kwok, and Y. Wang, "Using the discrete wavelet frame transform to merge Landsat TM and SPOT panchromatic images", Inf. Fusion, Vol. 3, No. 1, pp. 17–23, 2002
[18]. A.R. Sanjay, R.K. Soundrapandiyan, M. Karuppiah, and R. Ganapathy, "CT and MRI Image Fusion Based on Discrete Wavelet Transform and Type-2 Fuzzy Logic", International Journal of Intelligent Engineering and Systems, Vol. 10, No. 3, pp. 355-362, 2017.
[19]. H. Huang, X. Feng, and J. Jiang, "Medical Image Fusion Algorithm Based on Nonlinear Approximation of Contourlet Transform and Regional Features", Journal of Electrical and Computer Engineering, Vol. 2017, pp.1-9, 2017,
[20]. M. N. Do and M. Vetterli, "The contourlet transform: an efficient directional multi- resolution image representation", IEEE Transactions on Image Processing, Vol. 14, No. 12, pp. 2091–2106, 2005.
[21]. V. Bhateja, A. Srivastava, A. Moin, and A. Lay-Ekuakille, "NSCT based multispectral medical image fusion model", In: Proc. of the IEEE International Symposium on Medical Measurements and Applications, Benevento, Italy, pp. 1–5, 2016.
[22]. G. Bhatnagar, Q. M. J. Wu, and Z. Liu, "A new contrast based multimodal medical image fusion framework", Neurocomputing, Vol. 157, No.1, pp. 143–152, 2015.
[23]. Z. Y. Jin and Y. J.Wang, "Multi-modality medical image fusion method based on non- subsampled contourlet transform", Chinese Journal of Medical Physics, Vol. 33, No. 5, pp. 445– 450, 2016.
[24]. T. Z. Xiang, R. R. Gao, and L. Yan, "Multi-Scale fusion of infrared and visible images based on PCNN", Journal of Geomatics Science and Technology, Vol. 3, No.2, pp. 273–278, 2016.
[25]. G. Piella and H. Heijmans, "A new quality metric for image fusion," In: Proc. of the International Conference on Image Processing (ICIP '03), Catalonia, Spain, pp. 173–176, 2003.
[26]. H. Huang, X. Feng, and J. Jiang, "Medical Image Fusion Algorithm Based on Nonlinear Approximation of Contourlet Transform and Regional Features", Journal of Electrical and Computer Engineering, Vol. 2017, pp.1-9, 2017,
[27]. V. Bhateja, A. Srivastava, A. Moin, and A. Lay-Ekuakille, "NSCT based multispectral medical image fusion model", In: Proc. of the IEEE International Symposium on Medical Measurements and Applications, Benevento, Italy, pp. 1–5, 2016.

IOSR Journal of Electronics and Communication Engineering (IOSR-JECE) is UGC approved Journal with Sl. No. 5016, Journal no. 49082.

H.Devanna. " Evaluation of Quality Parameters for Medical Image Fusion." IOSR Journal of Electronics and Communication Engineering (IOSR-JECE) 14.2 (2019): 22-29.